Inertia emulation from HVDC links for LFC in the presence of smart V2G networks

12

*Sanjoy Debbarma**, *Rituraj Shrivastwa*†
*Electrical Engineering Department, NIT Meghalaya, Shillong, India, †Department of Electrical Power Engineering (IEE), Grenoble Institute of Technology, Grenoble, France

12.1 Introduction

The world is experiencing many challenges associated with the phasing out of natural resources such as coal and oil. One of the major solutions can be the integration of renewable power sources (RPS) such as solar photovoltaic (SPV) and wind energy to the grid. However, such intermittent sources will increase the unpredictability in the energy systems which in turn affect the grid frequency. It is well-known fact that any imbalance between total power generated and demanded in an interconnected power system affects the grid frequency and could results into blackouts if persist for a longer period of time. Power generation involving wind generator and SPV due to their variable output have more possibility of imposing stress on the power system. To maintain the equilibrium of power system, the balance between generation and load must be identical. Such balance can be maintained via automatic generation control (AGC) or load-frequency control (LFC) (Elgerd and Fosha, 1970). During abnormal situation, three tasks must be performed by the AGC mechanism: (1) grid frequency is to be maintained satisfactorily within permissible bounds, (2) any deviations in power flow through the tie-line between control areas must be zero, and (3) optimal generation must be done.

To deal with the frequency stability issue, speed governor is used through primary frequency control (PFC) loop. However, control action of such primary controller is inadequate to maintain the deviation and subsequently the secondary control technique is incorporated along with the governor. So far, many critical investigations pertaining to AGC or LFC have been studied. However, traditional way of controlling may not be suitable for modern power system with high penetration of RPS-based generation, DGs, and electric vehicle (EV) networks. It is interesting to mention that all the aforesaid sources and EV infrastructure involves the power electronic devices when connected to grid (Zhu et al., 2014). A typical modern power system is shown in Fig. 12.1 consisting of RPS, V2G networks and conventional units. It is well-known fact that massive integration of RPS, inspired by sustainability concerns, would present several challenges to power system control and operation.

Smart Power Distribution Systems. https://doi.org/10.1016/B978-0-12-812154-2.00012-2

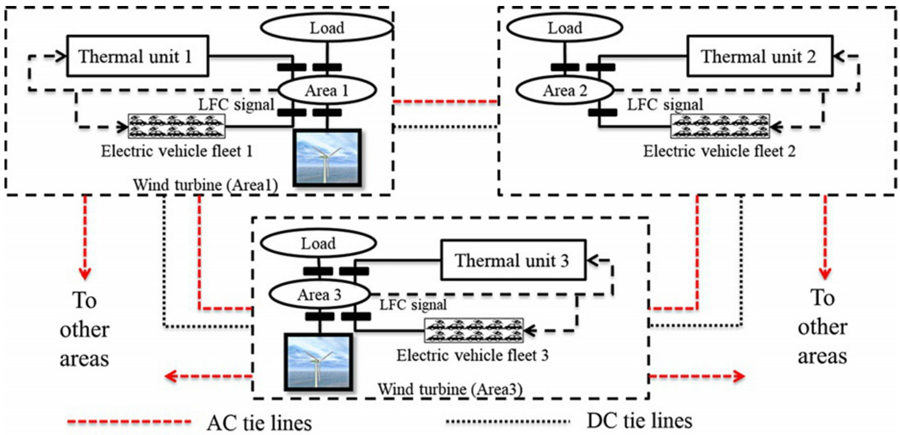

Fig. 12.1 Typical interconnected power system with RPS penetration and V2G network.

Also, the increasing penetration of RPS like wind power and PV generation may act to worsen the grid frequency stability due to lack of sufficient inertia. Traditionally rotational inertia to the power systems are provided by synchronous generators (SGs) (Castro and Acha, 2016). Undoubtedly, such low-inertia grid with power electronics converters (due to integration of RPS) presents a greater risk of instability requiring alleviation like changes to dispatch control systems, necessity for considerable amounts of spinning reserve and recurrent starting of conventional generators, which is often inefficient, challenging and costly from the business point of view. In many countries, RPS-based generations is interfaced with high-voltage direct current (HVDC) transmission lines due to attractive advantages such as fast frequency support, bidirectional controllability, and power oscillation damping. However, such modern power system with increasing electronically interfaced components due to HVDC systems and integration of RPS would suffer from lack of physical inertia and damping response which in turn put negative impacts on frequency regulation (FR) (Rakhshani et al., 2017). This is a trouble which demands crucial research investigation, as power networks with poor inertia are probably to become more common. To address these, many recent researchers designed methodology of emulating virtual inertia using the short-term energy storage system (ESS). In Zhu et al. (2014), inertia emulation controller (INEC) framework is implemented for contributing inertia by a DC link in voltage source converter (VSC)-based multiterminal DC (MTDC) system. Rakhshani et al. (2016a,b) focused on emulating the inertia using derivative of frequency signal for HVDC systems. But both the works used derivative of frequency signal for inertia emulation are very sensitive to noise and affect the system stability. Subsequently, concept of synchronous power controller (SPC) is implemented in converter station of HVDC links for inertia emulation (Rakhshani et al., 2017). The advantage of the SPC concept over other aforesaid methods is that it does not use phase-locked loop (PLL) for estimation of the signals. In other words, this method is a PLL-less concept for grid synchronization.

In most of the inertia emulation technique, DC link is treated as ideal battery source with immense storage which practically may not be (Ashabani and Mohamed, 2014). Therefore, an additional huge energy reserve is required to reduce the risk of instability on the power system. In smart grid environment, contribution from mobile vehicles can be one of the possible cost effective solutions for LFC problem (Pillai and Bak-Jensen, 2011). Recently, EVs are being adopted increasingly as it can alleviate effect to urban heat island to help local as well as global climates. It is found that, in practice, most of the EVs with onboard battery pack are parked in idle condition for several hours per day (Yilmaz and Krein, 2012, 2013). Besides acting as a load, EVs can also take part in PFC and secondary frequency control (SFC) through vehicle-to-grid (V2G) infrastructure (Debbarma and Dutta, 2017). More details on EV networks participating in LFC- and SPC-based HVDC transmission links are presented in the succeeding sections.

12.2 Inertia emulation from SPC-based HVDC systems for LFC

As discussed earlier, converter interfaced generators would invite negative impacts on future power systems by reducing the physical inertia, thereby imposing threat to power system stability. It is well-known fact that the kinetic energy stored in the rotating machines is responsible for counteracting any mismatch through inertial response until PFC activates. Now the question is how to compensate for reduced inertial response in future low-inertia power system. A probable solution is to improve the dynamics of the converters by specifying the properties of the grid-connected converters in such a way that it acts like a SG (Rakhshani et al., 2017). Although there exist different methods for inertia emulation, but all the techniques depends on PLL concept for measurement and estimation. Such amplified noise caused by frequency deviation measurements could bring instability problems (Rakhshani et al., 2016a,b). This limitation can be even worse, especially during abnormal faults and unsymmetrical system. In this section, the mathematical modeling of HVDC transmission system using SPC idea is presented for virtual inertia emulation. The principle idea is based on the control of VSC of HVDC link via active power loop and virtual admittance. Now, before modeling SPC-based HVDC transmission model, let us derive the conventional small signal model of HVDC link. With conventional small signal model of HVDC links incorporated in parallel with the HVAC transmission links, $\Delta P_{dci\text{-}j}(s)$ can be written as

$$\Delta P_{dci-j}(s) = \frac{K_{dci}}{1 + sT_{dci}} \Delta E_{dci}(s) \tag{12.1}$$

where K_{dci} represents feedback gain of HVDC tie-line, T_{dci} represents the time constant of HVDC tie-line, and ΔP_{dci-j} is direct current power deviation between area i and area j. Here, $\Delta E_{dci}(s)$ is the control error and can be represented as

$$\Delta E_{dci}(s) = \left[K_{fi}\Delta f_i(s) + K_{fj}\Delta f_j(s) + K_{ac}\Delta P_{tiei-j}\right] \tag{12.2}$$

where Δf_i and Δf_j are the frequency deviation in area i and area j where $i \neq j$. K_{fi}, K_{fj}, and K_{ac} are control gains of power modulation controller (PMC). With this new state in HVDC systems, area control error (ACE) will be reconstructed as follows:

$$ACE_{newi} = \left[\Delta f_i \beta_i + \Delta P_{totali-j}\right] \tag{12.3}$$

$$\Delta P_{totali-j} = \Delta P_{dci-j} + \Delta P_{tiei-j} \tag{12.4}$$

where $\Delta P_{totali-j}$is total tie-power line deviation. It is significant to mention that SPC loop in HVDC imitate the response of SG here but not fully; however, it demolishes the limitation of oscillatory response of SG (Rakhshani et al., 2017). The storage element such as capacitor between two converter stations in DC link can be modeled in the converter topology. The most advantageous feature of this SPC strategy is that any storage devices can be used alongside the converters to supply the deficit in the grid. Fig. 12.2 shows the active SPC loop used in modeling of HVDC systems. This loop consists of electromechanical block and virtual admittance-based converter block and can be obtained by reconstructing the second-order swing equation of SG.

In active SPC loop, P_i and P_o is the input power and the output power of converter, respectively, variation of which (ΔP) is the input to power loop controller (PLC). The mathematical model of PLC shown within the electromechanical block depicts the rotational behavior of SG and can be represented as

$$PLC(s) = \frac{\omega_n^2 / P_{Active}}{s + 2\zeta\omega_n} \tag{12.5}$$

where ω_n and ζ are the natural frequency and damping factor, respectively. P_{Active} is the delivered maximum active power. Here, PLC fixed a relative rotor frequency which append with synchronous speed of grid (ω_s) to give virtual rotor frequency of electromotive force (ω_r). Integration of ω_r enables the measurement of phase angle (θ_r) of virtual rotor which after subtracting from grid voltage angle (θ_{grid}) provide load

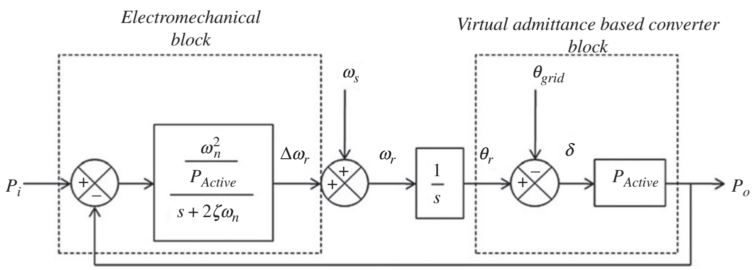

Fig. 12.2 SPC active loop for HVDC system.

angle (δ), that is, angle between grid voltage and virtual emf. Therefore, the final active power equation of the SPC is given as

$$P_o = P_{Active}{}^{*}\delta \tag{12.6}$$

where $P_{Active} = EV/X$, wherein E and V is virtual electromotive force and grid voltage, respectively. Here X represents reactance due to virtual admittance. Output power of SPC can be easily adjusted by changing appropriately the angle of output voltage of the converter. Thus the complete transfer function of the loop can be obtained as

$$\frac{P_o}{P_i} = \frac{\omega_n^2}{s^2 + 2\zeta\omega_n s + \omega_n^2} \tag{12.7}$$

where

$$\omega_n = \sqrt{\frac{P_{Active}}{J\omega_s}} \quad \text{and} \quad \zeta = \frac{D}{2\sqrt{P_{Active}J.\omega_s}} \tag{12.8}$$

Here, D and J stand for damping constant parameter and moment of inertia, respectively. In Eq. (12.8), the proper selection of value of D and J could help to imitate the desired damping effect. Finally, for ith area power system scenario with SPC-based HVDC system, the control error in Eq. (12.2) can be rewritten as

$$\Delta E_{SPC,dci}(s) = \left[K_{SPC,fi}\Delta f_i(s) + K_{SPC,fj}\Delta f_j(s) + K_{SPC,ac}\Delta P_{tiei-j}\right] \tag{12.9}$$

where $\Delta E_{SPC,\ dci}(s)$ is the DC reference error signal and act as an input to SPC-based HVDC control whose output signal is $\Delta P_{SPC,\ dci-j}(s)$. For multiple HVDC links, the output power of DC link can be written as

$$\Delta P_{dci-j}(s) = \Delta P_{SPC,dci-j}(s) = \sum_{\substack{i=1 \\ i \neq j}}^{k} \Delta P_{SPC,dci-j} \tag{12.10}$$

where k is multiple SPC-based HVDC stations.

A SPC or virtual synchronous power (VSP) based concept is a PLL less concept for grid synchronization and considered as a good solution for the renewable generation systems with energy storage. Compared with the well-known virtual impedance structure, the virtual admittance structure emulates the output impedance without leading to the difficulties in implementation. The main advantages lay on the effectiveness for the complete range of harmonic frequencies and the simplicity in the inner loop implementation (Tamrakar et al., 2017). In this concept, the proposed control law reproduces basically the swing equation of a SG. The transmitted active power is increased or decreased by shifting the output voltage phase of the converter forward or backward. By regulating this power, the system automatically maintains the synchronization.

12.3 Introduction to V2G network

12.3.1 EV product and services for FR

Introduction of V2G technology offer EVs to participate in different ancillary services under competitive electric market. EVs provide an opportunity to grow new products and services for grid management. As a one type of distributed energy storage, EVs is highly expected to play a vital role for emergency reliability services such as FR (Liu et al., 2015). On the other hand, EVs are gaining popularity because of reduced dependence on petrol and greenhouse emissions thus contribute to clean environment. As per the report, China has planned to put 200 million EVs by 2050 (Vachirasricirikul and Ngamroo, 2014). It is found that average personal vehicles travel on the road is nearly 4%–5% of the time, sitting in home garages or parking lots the rest of the day (Yilmaz and Krein, 2012). In an area, thousands of EVs can be aggregated to discharge active power to grid if there is a change/mismatch in power demanded and generated and help conventional units to meet the requirements instantaneously. Thus, EVs can participate in PFC as well as in LFC through V2G infrastructure. The charging and discharging of battery of the EV owners during peak and normal hours can be smartly controlled by new for-profit entity called EV aggregator with proper strategy.

As analysis of EV capabilities, several products or services are recommended for initial deployment based on a combination of their potential usefulness to the ISO or regional transmission organization (RTO) and the likely response from aggregators and end consumers (IRC, 2010). In the phased implementation approach, the initial products and services are indicated by minimum infrastructure required and support of grid reliability. They include (as per IRC, 2010):

1. Emergency load curtailment (ELC)—EVs are able to provide a quick response load-curtailment resource for emergency events and may be aggregated for the maximum effect. Due to relatively simple mechanisms for engaging this resource, and the large benefit of doing so, ELC of EV charging is a likely near-term product. It could serve in a reliability-based or economic demand response (DR) capacity.
2. Dynamic pricing (DP)—DP might be a solution to accomplish charging of EV batteries in off-peak hours. Nonetheless, research on consumer behavior is important to understand how an EV owner will respond to retail price differentials. In addition, EV-specific DP may be one way to introduce DP to consumers while avoiding political sensitivities regarding DP for existing retail loads.
3. Enhanced aggregation (EA)—The potential for high concentrations of EV loads in the evening makes managing charging over the day a priority for the ISO/RTOs. Some aggregators, automakers, and information management groups appear to be proactive in developing scheduling capabilities, possibly using additional information provided by the ISO/RTO. This product would be complementary to planned time-of-use (TOU) programs typically offered by the retail utilities. It also could be potentially linked to a DP product.

When V2G infrastructure is installed in the existing distribution networks, the following market products can provide value to the ISO/RTOs and aggregators:

1. Regulation—Expected EV loads in the next few years will not likely have a large impact on the amount of total regulation in the ISO/RTO markets or on regulation market prices. However, the regulation market is attractive to EV stakeholders since it can generate fairly predictable revenues. In addition, the relatively simple but new communication requirements for this product make it a good trial for subsequent EV products and services.
2. Reserves—EVs are able to provide reserve resources with relatively simple control of EV charging. Furthermore, this product appears to complement upcoming developments in DR resources as a result of smart grid developments.

For EV aggregators to participate in wholesale electric markets, firstly, ISO must ensure that aggregators have the capability to identify EVs location. Then aggregator purchases the power by engaging themselves in the day ahead market, which later will resell to the EV owners at predetermined price. The function of aggregator is to collect the information of the status of EVs and send it to the control operator. EVs receive the control signal from the operator and update their data/information in real time. Such information may be state of charge (SOC), EVs' capacity, numbers of EVs plugged in to charging station and future driving demand. For bidirectional power flow, that is, for charging and discharging of EVs, an active grid connected bidirectional AC-DC converter that enforces active power factor correction, and a bidirectional DC-DC converter to regulate the battery charge or discharge current is required. When operating in charge mode, the charger should draw a sinusoidal current with a defined phase angle to control power and reactive power. In discharge mode, the charger should return current in a similar sinusoidal form. However, incorporating bidirectional power flow has many challenges as well; viz. battery degradation due to frequent charging and discharging regulation, extra costs for bidirectional converters, metering issues, proper forecasting of EV reserve and driving behavior, interface concerns, etc.

Fig. 12.3 shows a schematic diagram of three area multisource interconnected power systems where in each area EVs are connected to the grid using V2G network. In such power grid, communications must be bidirectional to report battery status and receive commands such that the grid as well as the EVs can send each other economic and control signals. This will help in tracking intermittent resources and alter charge rates to track power prices, frequency or power regulation, and spinning reserves. A variety of communication protocols have to be studied for this purpose, including ZigBee, Bluetooth, Z-Wave, etc. and choose the best one for the purpose. Furthermore, in order to maintain proper safety isolation is important. It is beneficial for EV functions, including the high-voltage battery, DC-DC converter, traction inverter, and charger. Galvanic isolation in EV supply equipment can be provided either with a line transformer or in the DC-DC converter stage with a high-frequency transformer. High-frequency transformer isolation supports voltage adjustment for better control, safety for load equipment, compactness, and suitability for varying applications.

12.3.2 Modeling of LFC system with V2G energy network and SPC HVDC links

For power pool operation, grid frequency must be managed in acceptable bound to support generation-load balance. Such mechanism is attained by centralized LFC/AGC. Any imbalance between supply demand is represented by ACE signal given by Eq. (12.11)

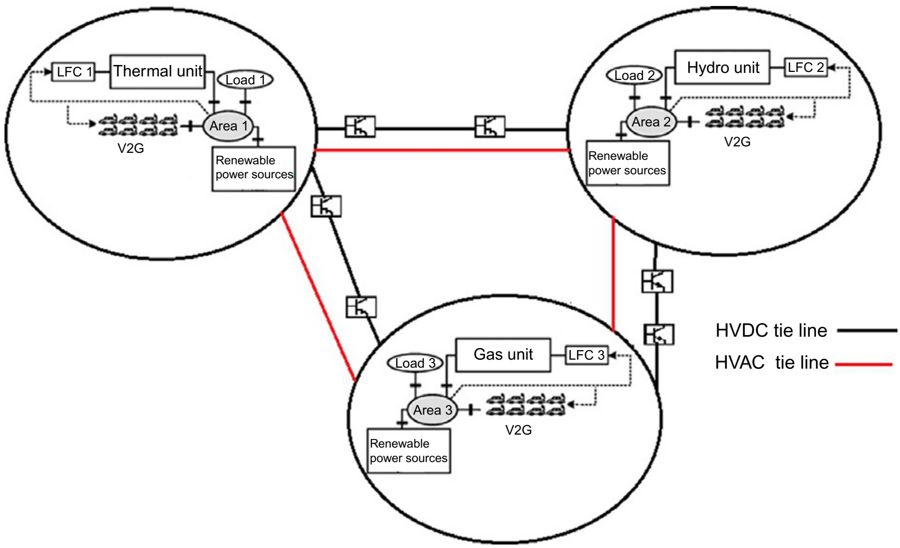

Fig. 12.3 Schematic diagram for three area system with V2G networks (Debbarma and Dutta, 2017).

$$ACE_i = \left[\Delta f_i \beta_i + \Delta P_{tiei-j}\right] \tag{12.11}$$

where β is bias factor, Δf_i is frequency deviation, and $\Delta P_{tiei\text{-}j}$ is net tie-line power between two control areas. Minimization of ACE signal would provide good dynamics and ensure the stability power system. Fig. 12.4 shows the basic frame of ith control area with EV penetration, thermal unit, and SPC HVDC links. The output power of the different sources is controlled via PFC loop and secondary loop. T_{gi} is steam governor time constant, T_{ti} is steam turbine time constant, R_i is the governor speed regulation parameter, T_{pi} and K_{pi} is the power system time constant and gain. APF is called ACE participation factor of EV fleet and conventional unit.

V2G energy network owing to its huge energy reserve can contribute to LFC of power grid. EVs act as a prosumer because they can charge their battery by taking energy from grid as well as inject energy to the grid. However, power availability of V2G network is uncertain due to random arrivals and departures of EVs. If arrivals and departures of EVs between any two districts are same, they are considered as symmetrical. However, practical scenario is generally asymmetrical between the districts especially during rush hours which in turn affect the battery SOCs. Thus, to realize the asymmetrical EVs movement in simulation study one must define the increasing and decreasing figure of EVs for different time interval. Based on the driving behaviors of EV owner and their expected SOC level, three different types of EV fleets can be categorized.

1. *Type I*: This type of fleet is very common where EVs randomly arrives and depart round the clock. Here injection of V2G power from aggregator following ACE is not fixed as the number of EVs kept changing with time.

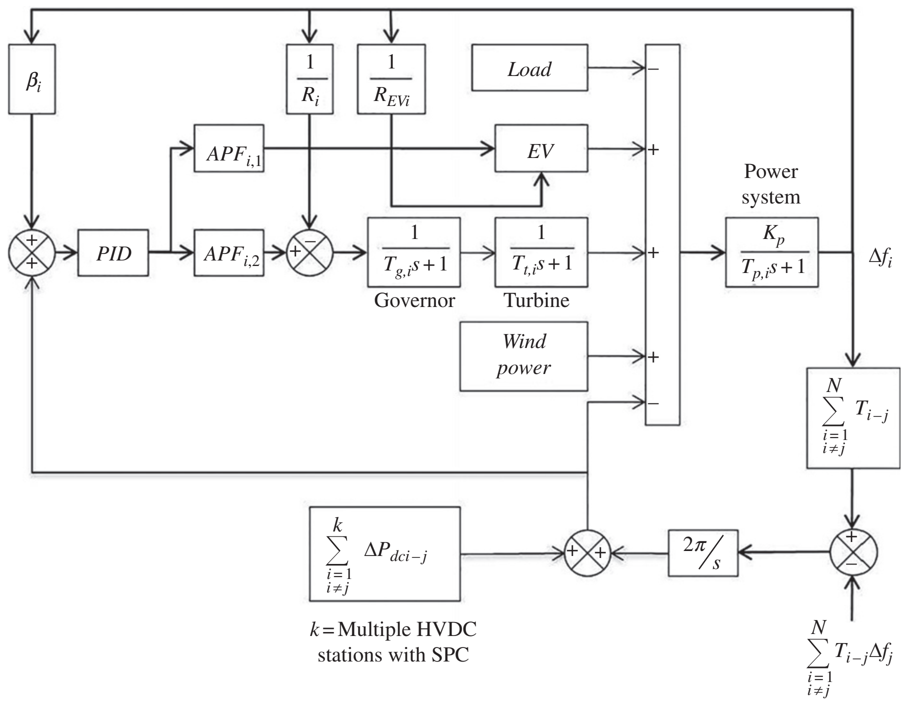

Fig. 12.4 Basic frame of *i*th control area with EV penetration and HVDC links.

2. *Type II*: In a lot of cases we may find that the EVs are parked in the garages for a longer period of time throughout the day. This type includes those EVs and the owners can sell the redundant power to the grid to earn revenues.
3. *Type III*: This type of the EVs includes those which come with the emergency requirement like charging and possess very low SOC.

EVs participating in FR can be defined based on smart balance SOC control technique as

$$P_{EVi} = \begin{cases} K_c{}^*ACE, & ACE \geq 0 \\ K_d{}^*ACE, & ACE < 0 \\ P_{AG}{}^{\max}, & K_c{}^*ACE \geq P_{AG}{}^{\max} \\ -P_{AG}{}^{\max}, & K_d{}^*ACE \leq -P_{AG}{}^{\max} \end{cases} \tag{12.12}$$

where P_{EVi} is output power of V2G fleet, $P_{AG}^{\max}$ and $P_{AG}^{\min}$ represents maximum and minimum value of V2G fleet power output, respectively. Here the charging (K_c) and discharging (K_d) coefficient are calculated based on Eqs. (12.13), (12.14), respectively.

$$K_c = K_{\max}\left\{1 - \left(\frac{SOC_i - SOC_{\text{low}}}{SOC_{\max} - SOC_{\text{low}}}\right)^n\right\} \tag{12.13}$$

$$K_d = K_{\max}\left\{1-\left(\frac{(SOC_i - SOC_r) - SOC_{high}}{SOC_{\min} - SOC_{high}}\right)^n\right\} \tag{12.14}$$

where $K_{\max}$ is the maximum EV gain, SOC_{high} and SOC_{low} is the high and low SOC, respectively, $SOC_{\min}$ and $SOC_{\max}$ are the minimum and maximum SOC of the battery, respectively, and n is the specification of the designed battery SOC. In Eq. (12.14), SOC_r is defined as reserved SOC required by EV owners for their upcoming driving. Any EV owners can set SOC_r value keeping in the view their next travel distance.

12.4 Simulation studies

12.4.1 LFC of power system with V2G control

Here, a three area interconnected system is considered as a study system which comprises conventional thermal units and V2G networks having capacity of 2000, 4000, and 8000 MW in area1, area2 and area3, respectively. Modeling of the test model is based on the Fig. 12.4 where both HVAC- and SPC-based HVDC tie-lines are connected in parallel. Parameters of the thermal systems, EV fleets and other are taken from Debbarma et al. (2014) and provided in Table 12.1. The model of the wind turbine system is designed (Nandar, 2013) and the corresponding output is shown in Fig. 12.5. In our study, it is assumed that only first and third control areas are penetrated with high wind power. EV fleets in all the areas is modeled considering only Type I and Type II fleets as discussed above with their initial SOC as 65% and 85%, respectively. Load perturbation is assumed to be occurred in all the areas simultaneously.

Fig. 12.6A and B shows the frequency deviation taken place in area1 and tie-line power deviation between area1 and area2. It is clearly seen that when only Type II EV fleets is considered, fluctuations is more as the reserve capacity of fleets changes. However, when Type I and Type II fleets are considered in the networks, dynamic response of frequency and tie-power significantly improved. Following error and wind power fluctuations, V2G algorithm updates the value of K_c and K_d. For analysis, value of parameters in Eqs. (12.13), (12.14) are taken as $SOC_{\min} = 10\%$, $SOC_{\max} = 90\%$, $SOC_{\text{low}} = 20\%$, $SOC_{\text{high}} = 80\%$, $SOC_r = 20\%$, and $n = 2$ (Vachirasricirikul and Ngamroo, 2014). The charging and discharging rate of the EV battery is taken as ±5 kW.

Table 12.1 Parameters of the three area system (Debbarma et al., 2014; Debbarma and Dutta, 2017)

Parameter	Value
f, T_{gi}, T_{ri}, T_{ti}, K_r	60 Hz, 0.08 s, 10 s, 0.3 s, 0.5
H_i, T_w, D_i,	5 s, 1 s, 0.00833 p.u. MW/Hz
T_{pi}, K_{pi}	20 s, 120 Hz/p.u. MW
R_i, R_{EVi}	2.4 Hz/p.u. MW, 2.4 Hz/p.u. MW
β_i, K_{EV}, T_{Evi}	0.425 p.u. MW/Hz, 1, 1 s
a_{12}, a_{23}, a_{13}	−1/2, −1/2, −1/4

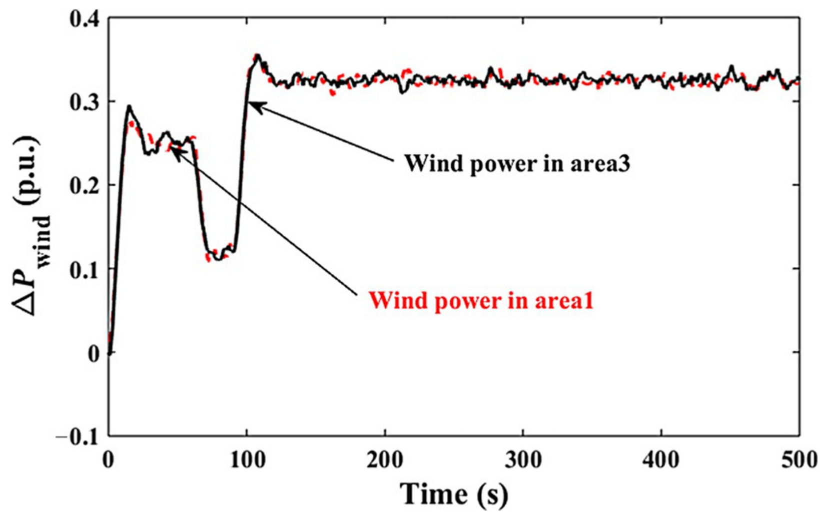

Fig. 12.5 Wind output power integrated to grid.

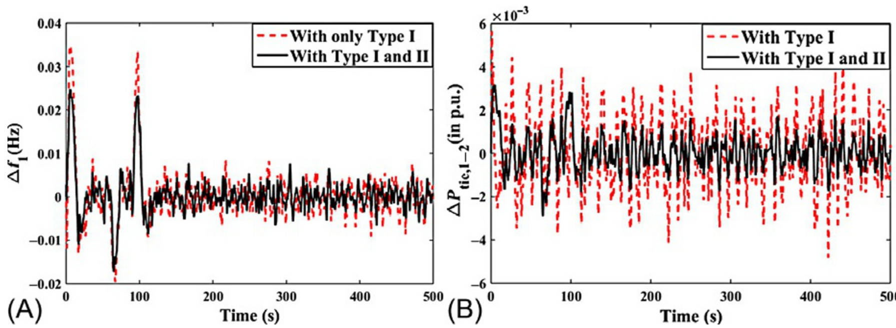

Fig. 12.6 (A) Frequency deviation in area1 and (B) tie-line power deviation between area1 and area2.

12.4.2 Inertia emulation from SPC HVDC transmission links of multiarea power system penetrated with V2G network and wind turbine systems

In this case, V2G network comprises all the types of EV fleets, that is, Types I, II, and III and control areas are interconnected via parallel HVAC- and SPC-based HVDC tie-lines. Same power system discussed above is considered for investigation. The main intension is to evaluate and show the positive impact of SPC-based HVDC links and EVs on grid frequency and tie-line power. The value of the parameters ζ and ω_n of SPC HVDC lines are taken as 1.31 and 6.87, respectively. For all the cases, parameters of the PMC and supplementary controller are tuned using cuckoo search algorithm.

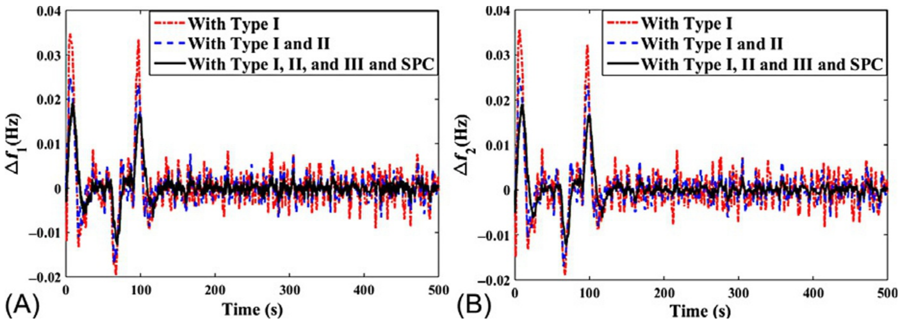

Fig. 12.7 (A) Frequency deviation in area1 and (B) frequency deviation in area2.

This is to mention further that any good optimization techniques can be used for selection of the optimum parameters of the controller. Eq. (12.8) can be used for calculating the related damping and the required inertia for SPC design. Fig. 12.7 represents the frequency deviation of a control area1 and control area2. It is clearly observed that the deviation corresponding to the case where all the EV fleets along with inertia emulation from SPC HVDC lines are not only suppressed and damped out to very low value but also remarkably curtailed the overshoot and undershoot. The quick recovery of the grid frequency is due to the contribution of the regulated V2G network and SPC-based HVDC transmission links. It is to be noted that proper selection of damping factor and inertia for HVDC system is very crucial for obtaining better result. More details on SPC HVDC can be studied from Rakhshani et al., 2017. In Fig. 12.8A, the dynamic response of emulated energy variation obtained from SPC-based DC system following load disturbance and wind variations is shown. The instantaneous response from HVDC links between the areas result into quick suppression of peak deviation and oscillations in dynamic response which undoubtedly shows the capability of SPC transmission system in emulating the virtual inertia. Fig. 12.8B shows the deviation in tie-line power exchanged between the area1 and area3.

In Fig. 12.9, SOC characteristics of V2G network in control area1 is shown. Type I fleet here is acting in a charging mode due to high surplus wind power. EVs in Type

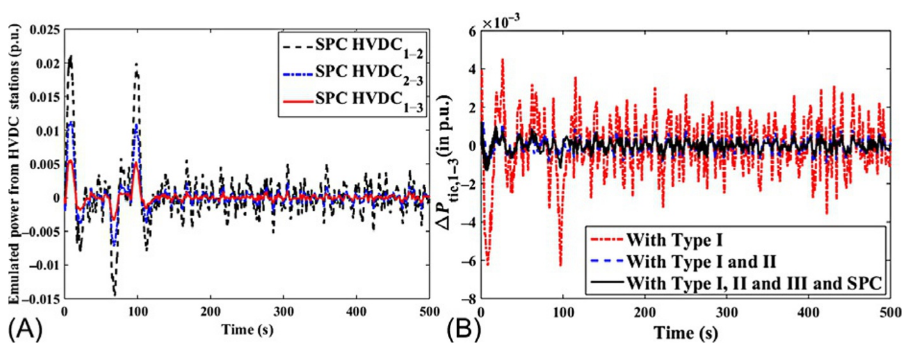

Fig. 12.8 (A) Variation in emulated power from SPC HVDC links and (B) tie-line power deviation.

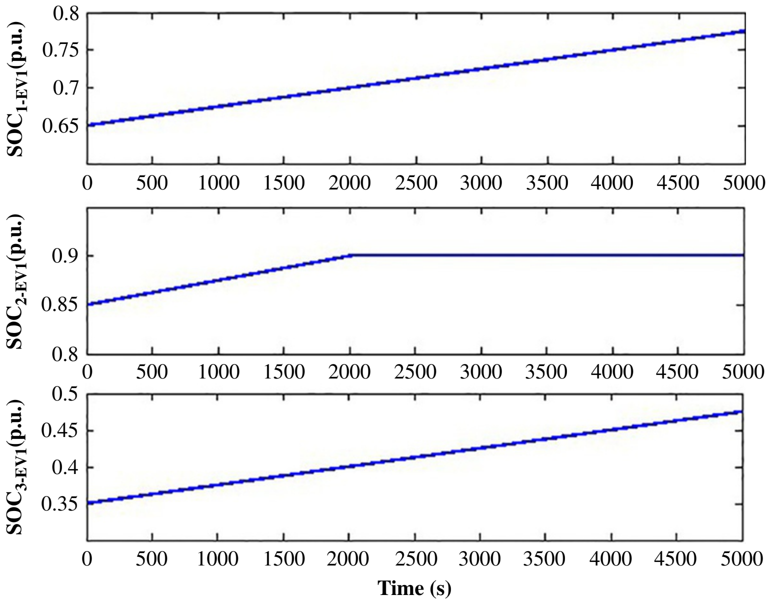

Fig. 12.9 SOC curve of Type I, II, and III fleets in area1.

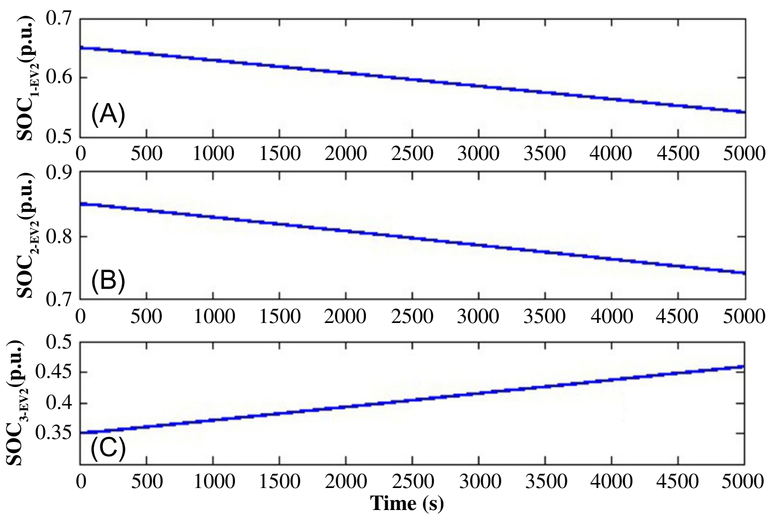

Fig. 12.10 SOC curve of (A) Type I, (B) Type II, and (C) Type III fleets in area2.

II fleet are charged up to their maximum limit, that is, 90% and ready for driving. Whereas Type III fleet owing to low SOC level continues to charge their batteries till the desired level is achieved. Fig. 12.10 is the SOC plots corresponding to the area2. It is seen that Type I and Type II EV fleets help to balance the power crisis (act in discharging mode) and assist thermal unit following perturbations. However, Type III is charging their batteries regardless of the grid condition for upcoming driving.

12.5 Conclusions

In this chapter, attempt has been made to analyze the cooperative control of V2G networks and SPC-based HVDC transmission systems for LFC in the presence of high wind penetration and conventional units. Based on the driving behavior of EV owners, V2G network for EVs participating in the LFC is designed which imitates real-time scenarios like random movement of EVs and upcoming charging demand. It has been found that the EV fleet responds fast unlike the conventional generation units. Modeling and contribution of SPC-based HVDC links is studied in details during load perturbations and variable wind power output. It is found that HVDC converter stations instantly provide inertia response following perturbation as well as wind output variation before thermal units react and diminish the peak deviations. Simultaneously based on ACE signal EVs react rapidly and assist in reducing the deviations and oscillations.

References

Ashabani, M., Mohamed, Y.A.I., 2014. Novel comprehensive control framework for incorporating VSCs to smart power grids using bidirectional synchronous-VSC. IEEE Trans. Power Syst. 29 (2), 943–957.

Castro, L.M., Acha, E., 2016. On the provision of frequency regulation in low inertia AC grids using HVDC systems. IEEE Trans. Smart Grid 7 (6), 2680–2690.

Debbarma, S., Dutta, A., 2017. Utilizing electric vehicles for LFC in restructured power systems using fractional order controller. IEEE Trans. Smart Grid 8 (6), 2554–2564.

Debbarma, S., Saikia, L.C., Sinha, N., 2014. Robust two-degree-of-freedom controller for automatic generation control of multi-area system. Int. J. Elect. Power Energy Syst. 63, 878–886.

Elgerd, O.I., Fosha, C.E., 1970. Optimum megawatt-frequency control of multi-area electric energy systems. IEEE Trans. Power Apparatus Syst. 89 (4), 556–563.

ISO/RTO Council (IRC), 2010. Assessment of plug-in electric vehicle integration with ISO/RTO systems.

Liu, H., Hu, Z., Song, Y., Wang, J., Xie, X., 2015. Vehicle-to-grid control for supplementary frequency regulation considering charging demands. IEEE Trans. Power Syst. 30 (6), 3110–3119.

Nandar, C.S.A., 2013. Robust PI control of smart controllable load for frequency stabilization of microgrid power system. Renew. Energy 56, 16–23.

Pillai, J.R., Bak-Jensen, B., 2011. Integration of vehicle-to-grid in the western Danish power system. IEEE Trans. Sustain. Energy 2 (1), 12–19.

Rakhshani, E., Remon, D., Cantarellas, A.M., Garica, J.M., Rodriguez, P., 2017. Virtual synchronous power strategy for multiple HVDC interconnections of multi-area AGC power systems. IEEE Trans. Power Syst. 32 (3), 1665–1677.

Rakhshani, E., Remon, D., Cantarellas, A.M., Rodriguez, P., 2016a. Analysis of derivative control based virtual inertia in multi-area high-voltage direct current interconnected power systems. IET Gener. Transm. Distrib. 10 (6), 1458–1469.

Rakhshani, E., Remon, D., Cantarellas, A.M., Garica, J.M., Rodriguez, P., 2016b. Modeling and sensitivity analyses of VSP based virtual inertia controller in HVDC links of interconnected power systems. Electr. Power Syst. Res. 141, 246–263.

Tamrakar, U., Shrestha, D., Maharjan, M., Bhattarai, B.P., Hansen, T.M., Tonkoski, R., 2017. Virtual inertia: current trends and future directions. Appl. Sci. 7 (7), 1–29.
Vachirasricirikul, S., Ngamroo, I., 2014. Robust LFC in a smart grid with wind power penetration by coordinated V2G control and frequency controller. IEEE Trans. Smart Grid 5 (1), 371–380.
Yilmaz, M., Krein, P.T., 2012. Review of benefits and challenges of vehicle-to-grid technology. IEEE Energy Conversion Congress and Exposition, pp. 3082–3089.
Yilmaz, M., Krein, P.T., 2013. Review of the impact of vehicle-to-grid technologies on distribution systems and utility interfaces. IEEE Trans. Power Electron. 28 (12), 5673–5689.
Zhu, J., Guerrero, J.M., Hung, W., Booth, C.D., Adam, G.P., 2014. Generic inertia emulation controller for multi-terminal voltage-source-converter high voltage direct current systems. IET Renew. Power Gener. 8 (7), 740–748.

Further reading

Debbarma, S., Saikia, L.C., Sinha, N., 2013. AGC of a multi-area thermal system under deregulated environment using a non-integer controller. Electr. Power Syst. Res. 95, 175–183.
Sasaki, T., Kadoya, T., Enomoto, K., 2004. Study on load frequency control using redox flow batteries. IEEE Trans. Power Syst. 19 (1), 660–667.
Yogarathinam, A., Kaur, J., Chaudhuri, N.R., 2017. Impact of inertia and effective short circuit ratio on control of frequency in weak grids interfacing LCC-HVDC and DFIG-based wind farms. IEEE Trans. Power Deliv. 32 (4), 2040–2051.
Zhong, Q.C., Weiss, G., 2011. Synchronverters: inverters that mimic synchronous generators. IEEE Trans. Ind. Electron. 58 (4), 1259–1267.